Spatially resolved luminescence investigation of AlGaAs/GaAs single quantum wires modified by selective implantation and annealing

Xingquan Liu,[a)] Wei Lu, Zhi Feng Li, Yi Dong Chen, and S. C. Shen
National Laboratory for Infrared Physics, Shanghai Institute of Technical Physics, Chinese Academy of Sciences, Shanghai 200083, People's Republic of China

Y. Fu and M. Willander
Physical Electronics and Photonics, Department of Physics, Fysikgrand 3, University of Goteborg and Chalmers University of Technology, S-412 96 Goteborg, Sweden

Hark Hoe Tan, S. Yuan, and C. Jagadish
Department of Electronic Material Engineering, Research School of Physical Science and Engineering, The Australian National University, Canberra, A.C.T. 0200, Australia

J. Zou and D. J. H. Cockayne
Electron Microscope Unit and Australian Key Center for Microscopy and Microanalysis, The University of Sydney, NSW 2006, Australia

(Received 15 June 1999; accepted for publication 27 September 1999)

Single $Al_{0.5}Ga_{0.5}As$/GaAs *V*-groove quantum wires (QWR) modified by selective implantation and rapid thermally annealing were investigated by spatially resolved microphotoluminescence (micro-PL). The PL from the necking region was clearly observed at room temperature. Optical properties of QWR and the adjacent quantum well structures were strongly degraded by the implantation. The recovery properties of the PL signals from all the structures were dependent on the implantation dose. A critical dose of $1\times10^{13}\,cm^{-2}$ was found for the selective implantation, over which the PL from the necking region could not be recovered. Also the blueshifts of QWR and the necking-region PL peaks were observed for all the annealed samples. This blueshift is caused by the interface intermixing, which is very useful to increase the confinement of carriers in QWR region for optoelectronic device applications. © *1999 American Institute of Physics.*
[S0003-6951(99)00847-5]

V-groove quantum wires (QWRs) have attracted much attention in recent years[1–5] due to the fabrication simplicity and device application prospect. The *V*-groove QWR is fabricated by direct epitaxial growth on *V*-grooved substrate. One important feature in this *V*-groove QWR structure is the rather complicated structures near the QWR because of the complicated growth mode near QWR region, where (100), (111), and (311) facets are brought together. Different growth modes compete very strongly with each other during growth, and this competition results in different kind of low dimensional structures, i.e., (111) quantum well (QWL), top (100) QWL, (100) QWR, and (311) necking region. The lateral confinement comes from lateral necking region.

In laser device application, selective implantation is usually used to disable the lateral (111) QWL and confine the current.[6] In selective implantation as shown in Fig. 1, the QWR region will not be directly affected by ions, while the other regions are degraded by the implantation. Since the implanted ion will spread in the material, the quality in the QWR region will be also affected by the implantation in high enough dose. In order to have good QWR device properties, one needs to keep the QWR to be in good quality. So it is important to study the influence of the selective implantation on the optical property of QWR.

In this letter the selective implantation effect with and without rapid thermal annealing (RTA) is investigated by the microphotoluminescence (micro-PL) measurement at room temperature, at which most of the devices operate.

GaAs(100) semi-insulating substrate was processed by standard photolithography and wet etching. 50 periods of 2 μm wide stripes with 2 μm spacing were used to get periodic 4 μm *V* grooves. After the pattern transfer, a sawtooth-type surface profile (about 2.5 μm depth) was formed by wet chemical etching (H_3PO_4:H_2O_2:H_2O=1:1:3) at 0 °C. The *V* grooves were aligned along [0-11] direction. The *V*-grooved substrate was cleaned with warm trichloroethylene, acetone, methanol, and then trim etched with H_2SO_4:H_2O_2:H_2O(=20:1:1) for 20 s. A 0.1 μm GaAs buffer layer was grown before 1 μm $Al_{0.5}Ga_{0.5}As$ layer. Nominated 1 nm GaAs well layer was deposited followed by a 0.1 μm $Al_{0.5}Ga_{0.5}As$ top barrier layer. 200 nm GaAs top layer was grown finally. All layers were grown at 750 °C. Figure 1(a) shows the structure schematically. The QWR cross sections by transmission electron microscopy (TEM) for as-grown samples is shown in Fig. 1(b). The dark vertical band is formed at the bottom of the *V* groove as a low Al composition AlGaAs band due to the longer migration length of the Ga atom than the Al atom, and this low Al composition AlGaAs band form a vertical quantum well (VQWL).

Self-aligned dual implantation technique was used to selectively intermix the sidewall QWL with arsenic at 350 keV and at four different doses: 4×10^{11}, 1×10^{12}, 4×10^{12}, and $1\times10^{13}\,cm^{-2}$ respectively at room temperature. The implantation process was described in Ref. 5. Part of the implanted and as-grown samples were rapid thermally annealed at

a)Electronic mail: xqliu@isc.osakac.ac.jp

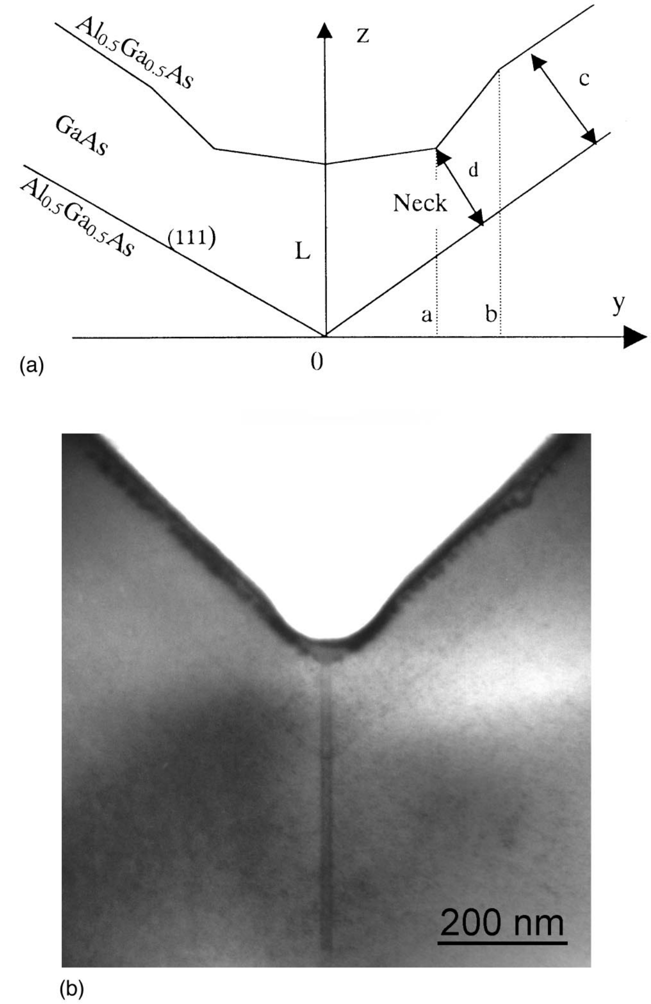

FIG. 1. (a) is the schematic of QWR structure, (b) is the TEM image graph of the QWR cross section.

900 °C in the rapid thermal annealer for 30 s. High spatial resolution Dilor-Super-Infinity analytic micro-Raman system was used to measure the micro-PL spectra of QWR samples at room temperature. The Ar^+ laser 514.5 nm line was used as excitation source. The diameter of laser spot is less than 1 μm. Five structures decomponented from PL spectra of as-grown sample at 1.743, 1.777, 1.884, 1.962, and 2.061 eV. Spatial mapping scanning across a single *V* groove shows that the 1.743 and 1.777 eV are from QWR. They are attributed to transition energy of first heavy and light hole sublevel to first electron sublevel $E_{1\mathrm{hh}-1e}$ and $E_{1\mathrm{lh}-1e}$ in QWR as described later. The peaks located at 1.884 and 1.962 eV co-exist with QWR PL in the spatial scanning. The peak at 1.884 eV is attributed to transitions of first heavy sublevel to first electron sublevel 1hh–1*e* in VQWL. But this peak has a high energy tail. This high energy tail is believed to be from the continue distribution of the Al mole composition from the GaAs region to the $Al_{0.5}Ga_{0.5}As$ barrier region. Then the peak at 1.962 eV is from 1hh–1*e* transition in the necking region. The peak at 2.061 eV can be observed in all regions of the sample. It is the interband transition of thick $Al_{0.5}Ga_{0.5}As$ barrier. The sidewall (111) QWL PL which is at 1.947 eV cannot be observed in the QWR region. Since we do our experiment at room temperature, the light hole sublevel is thermally occupied. It is reasonable that we can observe the PL signal from the recombination related with both the heavy hole and light hole in QWR.

TABLE I. *e*1–hh1 excitation energies [eV]. The geometric parameters of the quantum wire system are: $L=2$, $c=0.8$, $a=15$, $b=30$, $d=8.2$ nm. The Al mole fraction in the VQWL region is 0.35. $E_g(\mathrm{GaAs})=1.4224$ eV.

Spatial region	*e*1	hh1(lh1)	*e*1–hh1(lh1)	Exp.
QWR(*e*1–hh1)	0.2417	0.0830	1.7471	1.743
QWR(*e*1–lh1)	0.2417	0.14322	1.80732	1.777
Neck	0.3856	0.1625	1.9705	1.962
QWL	0.3651	0.1589	1.9464	1.946
VQWL	0.2984	0.1550	1.8758	1.884
$Al_{0.5}Ga_{0.5}As$			2.0455	2.061

The effective mass approximation was used to calculate the electronic structures in the *V*-groove QWR structure.[7] Since the QWR is not translational symmetric, we apply the recursion method (described in detail in Ref. 7) to solve two-dimensional schrodinger equation (cross section of QWR structure). In our calculation, we take the parameters as follows: $E_g(\mathrm{GaAs})=1.4224$ eV. $\Delta E_c=1.247\times 0.65x$ eV, $\Delta E_v=1.247\times 0.35x$ eV. $m_c=0.067$. Figure 2 shows the local density of states in the area of QWR, VQWL, and necking region. We take the Al composition in the VQWL region as $x=0.35$, the VQWL width 16.4 nm, wire lateral width 15 nm, and the thickness at crescent center 2 nm from TEM image graph [Fig. 1(a)]. In our model the Al composition was simply supposed same in the whole VQWL region, and was evaluated according to the PL experimental results. The calculated transition energies and experimental results are listed in Table I.

From Fig. 2 we find that there is only one confined electron state in the QWR. From the theoretical calculation, the 1.962 eV is from the necking region. The luminescence from the necking region is clearly observed at room temperature, also the QWR PL is very strong at room temperature.

Based on our good understanding of PL spectra of the *V*-grooved QWR sample, we study the selective implantation effect on optical properties of the QWR structures. The selectively implanted samples with and without RTA were measured by micro-PL. The PL spectra at the wire region are shown as in Fig. 3. All dots are experimental data and solid

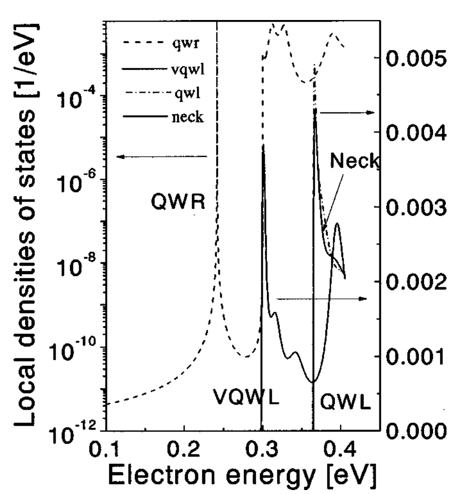

FIG. 2. Local density of states in the area of the QWR, VQWL, sidewall(111) QWL, and quantum well necking region (Neck).

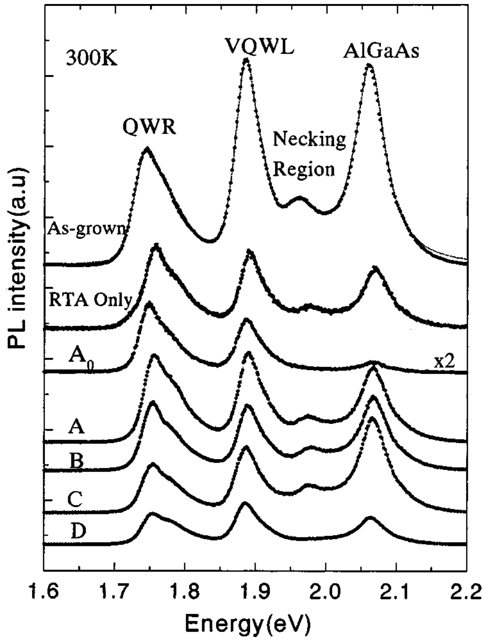

FIG. 3. PL spectra of all samples. The RTA only spectrum is the rapid thermally annealed as-grown sample. A_0 is the implanted sample at dose $4\times10^{11}\,\mathrm{cm}^{-2}$ without RTA, A, B, C, and D are spectra of implanted and annealed samples at doses of 4×10^{11}, 1×10^{12}, 4×10^{12}, and $1\times10^{13}\,\mathrm{cm}^{-2}$, respectively.

lines are fitting curves. RTA only line is PL of rapid thermally annealed as-grown sample. A_0 is the implanted sample at implantation dose of $4\times10^{11}\,\mathrm{cm}^{-2}$ without RTA. A, B, C, and D are implanted and annealed samples. For sample A_0 the PL signal from the necking region quenched and the PL intensity of all structures decreases. PL intensity of $Al_{0.5}Ga_{0.5}As$ barriers dramatically decreased because of the damage introduced by the implantation. The obvious decrease of the PL intensity of QWR and VQWL results from the decrease of carrier number feeding in from the $Al_{0.5}Ga_{0.5}As$ barrier. Two factors contribute to the quenching of necking region PL, one is damages in sidewall trap most of the carriers in sidewall (111) QWL, therefore, the number of thermally populated carriers from sidewall (111) QWL decreased dramatically, on the other hand the carriers in the necking region are rapidly captured by the damage center through the channel of sidewall (111) QWL, and also transports to the QWR region, the ratio of recombination in the necking region become very small.

The decreasing amount of PL intensity relative to as-grown sample for QWR and VQWL (3/4, 7/8, respectively) shows the source of the carriers in QWR and VQWL. The carriers in VQWL mainly come from the sidewall $Al_{0.5}Ga_{0.5}As$ barrier (approximately 7/8 of total carriers) besides stimulated *in situ*. In QWR, the carriers mainly come from the regions of VQWL, $Al_{0.5}Ga_{0.5}As$ barrier through VQWL, sidewall (111) QWL by tunneling through the necking region, and necking region besides *in situ* stimulated carriers. When sidewall $Al_{0.5}Ga_{0.5}As$ barrier and (111) QWL are damaged, about 3/4 of the total carriers are lost. The left 1/4 are mainly from VQWL and *in situ* stimulated carriers. This shows the role of VQWL in *V*-groove QWR structures.[8] From the earlier investigation, it is clearly shown that the selective implantation will effectively decrease the carrier transfer ability in the sidewall barrier and QWL. It is expected in the laser application.

The lines A, B, C, and D in Fig. 3 show the PL spectra of implanted and annealed samples. From Fig. 3 the PL intensity of all the structures recovered to some extent compared with implanted only samples, however, RTA cannot recover the optical properties completely. The necking region PL can be recovered for A, B, and C samples, but when the implantation dose is increased to $1\times10^{13}\,\mathrm{cm}^{-2}$, the PL signal cannot be recovered any more. The unrecovered defects in sidewall QWL and those getting into the necking region act as carrier trapping centers. This kind of defect-induced PL quenching behavior can be used to reflect the limitation of implantation doses when the selective implantation is used in laser device. From our study, when the As ion implantation dose is higher than $1\times10^{13}\,\mathrm{cm}^{-2}$, the QWR quality may start to degrade.

In Fig. 3, a small blueshift is observed for the QWR and necking region PL of all implanted and annealed samples compared with as-grown and implanted only samples. Maximum energy shifts for the QWR and necking region are 14 and 17 meV, respectively.

In summary, single $Al_{0.5}Ga_{0.5}As/GaAs$ *V*-groove QWR modified by selective implantation and RTA was investigated by micro-PL. The interband transitions related with the light and heavy hole are experimentally observed and theoretically analyzed for the QWR and its neighbor region. The PL signal from the necking region quenched for the implanted-only sample at dose of $4\times10^{11}\,\mathrm{cm}^{-2}$. RTA can recover the PL signal of the necking region. The unrecoverable quenching of the PL signal from the necking region with implantation doses increased to $1\times10^{13}\,\mathrm{cm}^{-2}$ may give the As implantation dose range of $4\times10^{11}-1\times10^{13}\,\mathrm{cm}^{-2}$ for laser device application at our implantation conditions.

This work was supported by a grant for State Key Program for Basic Research of China. The authors would also like to thank the financial support of Australian Agency for International Development (AusAID) through IDP Education Australia under Australia-China Institutional Links Program. X. Q. L. thanks the financial support of Shanghai ''QiMingXing'' Fund No. 98QA14004. H.H.T., S.Y., and J.Z. acknowledge the fellowship awarded by the Australian Research Council.

[1] E. Kapon, D. M. Hwang, and R. Bhat, Phys. Rev. Lett. **63**, 430 (1989).
[2] J. F. Ryan, A. C. Maciel, L. Rota, K. Turner, J. M. Freyland, U. Marti, D. Martin, F. Morier-Gemoud, and F. K. Reinhart, Phys. Rev. B **53**, R4225 (1996).
[3] Y. Kim, S. Yuan, R. Leon, C. Jagadish, M. Gal, M. B. Johnston, M. R. Phillips, M. A. Stevens Dalceff, J. Zou, and D. J. H. Cockayne, J. Appl. Phys. **80**, 5014 (1996).
[4] X.-L. Wang, M. Ogura, and H. Matsuhata, Appl. Phys. Lett. **66**, 1506 (1995).
[5] X. Liu, W. Lu, X. Chen, S. C. Shen, H. H. Tan, S. Yuan, C. Jagadish, M. Johnston, D. Lap, M. Gal, J. Zou, and D. J. H. Cockayne, 1998 Conference on Optoelectronic and Microelectronic Materials and Devices, Perth, Australia.
[6] R. Bhat, E. Kapon, D. M. Hwang, M. A. Koza, and C. P. Yun, J. Cryst. Growth **93**, 850 (1988); E. Kapon, S. Simhony, R. Bhat, and D. M. Hwang, Appl. Phys. Lett. **55**, 2715 (1989).
[7] C. Kiener, L. Rota, A. C. Maciel, J. M. Freyland, and J. F. Ryan, Appl. Phys. Lett. **68**, 2061 (1996).
[8] Y. Fu, M. Willander, X. Q. Liu, W. Lu, S. C. Shen, H. H. Tan, S. Yuan, and C. Jagadish (unpublished).